Palladium catalyst on anodized aluminum monoliths for the partial hydrogenation of vegetable oil

Jhon F. Sánchez M, Diego E. Boldrini, Gabriela M. Tonetto*, Daniel E. Damiani

PLAPIQUI (UNS-CONICET), Camino La Carrindanga Km 7, Bahía Blanca, CP 8000, CC 717, Argentina

ARTICLE INFO

ABSTRACT

The present work explores the viability of introducing improvements to the conventional process of hydrogenation using structured catalysts. Monolithic catalysts of anodized aluminum were prepared and characterized. They were impregnated with palladium and used as monolithic stirrers in the sunflower oil hydrogenation reaction at 100 °C and 413 kPa.

The monolithic catalysts showed to be active, with a 50% C=C conversion in 30 min. When consecutive tests were performed, a loss of activity was observed, decreasing 80% in the sixth test, which is attributed to the presence of carbonaceous residues.

© 2011 Elsevier B.V. All rights reserved.

1. Introduction

The hydrogenation of vegetable oils is a chemical process by which hydrogen is added to a carbon–carbon double bond in the glycerides of an oil molecule. The reaction takes place in the presence of a catalyst, usually nickel, and the product is an oil of higher consistency, stability and oxidation resistance [1]. These characteristics are required by the food production industry.

In recent years, there has been a growing interest in finding non-edible applications of vegetable oils, mainly due to their availability and environmental compatibility. Polyunsaturated vegetable oils used as biolubricants and alternative fuel must be treated in order to improve their resistance to oxidation by partial hydrogenation [2,3].

Industrially the process is carried out in tanks with conventional blade stirrers, hydrogen bubbling and the catalyst particles in suspension, usually working at 150–220 °C with pressures between 69 and 413 kPa, using a Raney Ni catalyst. The process is completed with a filtration system to separate the powder catalyst from the hydrogenated oil, and a bleaching step to remove metal traces from the finished product. Since the catalyst is part of the filter cake, part of the catalyst must be replenished in each oil batch to be processed. These filtration and bleaching procedures require time and are very expensive, representing approximately 20% of total operation costs [4].

An alternative designed to simplify the oil hydrogenation process and reduce its costs is the use of structured catalysts, ceramic and metal monoliths. The use of these catalysts would allow to remove the filtration step, which is very interesting both from an economic and environmental point of view. The application of monolithic catalysts would make more affordable the use of noble metals that are more active and/or selective than nickel, such as Pd or Pt [5–7]. Since noble metals are expensive, an efficient reuse of the catalyst is required [8,9], and structured catalysts are suitable to that end. It can also be mentioned that the subsequent metal extraction from the spent catalyst is easier in the case of noble metals than Ni, lowering the overall cost associated with these catalysts. In the case of Ni-based catalysts, only about 10% of the financial value of the Ni can be recovered by selling the spent catalyst after its use, whereas up to 95% of the noble metal content can be recovered and reused during the manufacture of fresh catalysts [10].

Moreover, Pd or Pt based-catalysts, due to their high activity, can operate at lower reaction temperatures (80–120 °C) than Ni during the hydrogenation of vegetable oils. Another operational benefit of using Pd is its lower reduction temperature, which would allow to perform the pre-treatment *in situ*, making the application of the monolithic stirrer to existing commercial equipment at edible oil hydrogenation plants easy, simply with the interchange of the stirrer.

Ceramic monolith catalysts have been widely known in environmental applications with reactions in gas phase. Cordierite is generally used, because it suits well the requirements of the automotive industry [11]. The main reasons are its high mechanical strength, and high resistance to elevated temperatures and tem-

---

* Corresponding author. Tel.: +54 291 4861700; fax: +54 291 4861600.
E-mail address: gtonetto@plapiqui.edu.ar (G.M. Tonetto).

perature shocks due to its low thermal expansion coefficient [12]. This type of structured catalyst has also been used in reactions in liquid phase, and particularly in hydrogenation [13–15] and vegetable oil hydrogenation reactions [4,16–18]. Despite the wide use of cordierite, it presents limitations related to minimum wall thickness (for a correct extrusion), the low thermal conductivity of ceramic materials and their low resistance to impact. Its use in the oil hydrogenation reaction is limited since ceramics deteriorate with use.

Metal monoliths present important advantages over ceramic monoliths. Their preparation is cheap and affordable in small quantities, they have a better thermal conductivity, they present thinner wall thickness allowing a greater flow area, they have a higher mechanical resistance, and they allow a greater flexibility in the design [19,20].

The difficulty in the preparation of metal monoliths for the hydrogenation of oils lies in the fixation of the catalyst layer onto the metallic substrate. An inadequate coating process or a weak adherence between the substrate and the coating can cause the catalyst (support or active phase) to be stripped by the flow during its pass through the channels.

When the working temperature is moderate, as in the hydrogenation of edible oil, an interesting substrate to prepare metallic monoliths is aluminum. Aluminum has excellent mechanical and thermal properties to be used as structural material [21]. The anodization generates an alumina layer strongly adhered to the metallic substrate. Thus, a structured catalyst with the advantages of a metal monolith and with a layer that is resistant and compatible with the active phase is obtained [22].

In the present paper, the partial vegetable oil hydrogenation over an anodized aluminum monolith supported Pd catalyst in a monolithic stirrer reactor is discussed in detail.

Since one of the advantages of monolith catalysts is that they can overcome the difficulty in separating the powder catalyst from the liquid phase in the slurry reactor, the stability of the sample was carefully analyzed.

2. Materials and methods

2.1. Preparation of monolithic catalysts

Anodized aluminum monolith catalysts were prepared, using a commercial laminated pure aluminum as metallic substrate. The composition of the aluminum sheets is shown in Table 1.

The aluminum sheets were cut in pieces of 15 mm × 18 mm and 15 mm × 23.5 mm. After cutting, they were washed with water and soap, then with acetone, and finally dried to remove the impurities on the surface. The bigger piece was rolled using a mechanical devise made of two Nylon cogwheels.

The anodization technology was used to generate on the aluminum surface an alumina layer that will serve as support for the palladium catalyst. With a careful selection of the anodization conditions, it is possible to obtain a layer adequate to support the active phase [22].

Conditions for the anodization process:

Table 1
Chemical composition (wt%) of the commercial aluminum.

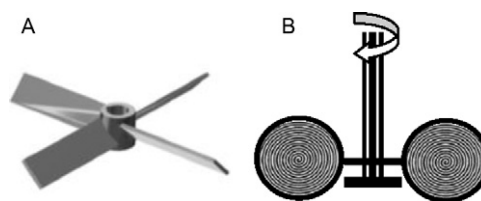| Metal	wt%	Metal	wt%
Al	0.5331	Zn	0.005
Fe	0.34	Mg	0.002
Si	0.10	Cu	0.002
Ti	0.011	Pb	0.001
Mn	0.005	Cr	0.0009

Fig. 1. Schematic views of the stirrers: (A) stirrer of inclined blades (used with the powder catalyst); (B) monolithic stirrer.

Electrolyte: oxalic acid, $H_2C_2O_4$
Electrolyte concentration: 1.6 M
Temperature: 40 °C
Flow density: 2 A/dm^3
Time: 40 min anodization + 40 min pore opening

Al_2O_3/Al monoliths were prepared by rolling around spindle alternate previously anodized flat and corrugated foils. The final monolith was a cylinder of 14 mm diameter by 15 mm height and a cell density of 350 cells per square inch (cpsi). The monoliths were loaded with Pd by wet impregnation, by dipping them in a $Pd(C_5H_7O_2)_2$ solution in toluene at room temperature for 24 h, under agitation. After impregnation, the monoliths were dried in N_2 at 150 °C for 2 h, and then calcined at 500 °C for 2 h. These samples will be referred to as Pd/Al_2O_3/Al.

2.2. Catalyst characterization

Textural properties were studied by N_2 adsorption–desorption isotherms at 196 °C in a Micromeritis ASAP 2020 apparatus between 0.1 and 0.995 mmHg with a home-made cell that allows complete monolith analyzing. Before analysis, the monoliths were degassed for 2 h at 150 °C in vacuum.

The morphology and thickness of the catalyst layer deposited on the monolith substrates were analyzed by scanning electron microscope (SEM) (JEOL 35 CF) and transmission electron microscopy (TEM) (JEOL 100 CX) operating at 100 kV.

The Pd content of the catalyst was determined by atomic absorption spectroscopy in a GBC AVANTA Σ spectrometer. Diffuse reflectance infrared Fourier transform spectroscopy (DRIFTS) spectra were recorded in a Nicolet 6700 FT-IR spectrometer in the 4000–400 cm^{-1} region. The spectra were recorded with a 4 cm^{-1} resolution and 64 scans using a high-sensitivity mercury cadmium telluride (MCT-A) detector. Silicon carbide disks (Si-Carb) were used to sample the surface layer of the monolith. A clean Si-Carb paper was used for the background. Sunflower oil and hydrogenated sunflower oil were dissolved in hexane and mixed with a proper amount of KBr. The solvent was evaporated completely and the powder analyzed.

The amount of alumina generated during anodization was determined by means of gravimetry. It was calculated from the weight difference of the anodized sheet before and after the chemical treatment which dissolved selectively the alumina layer. The dissolution process was carried out at 85 °C for 20 min using a 0.5 M phosphoric acid and 0.2 M chromic acid solution.

2.3. Catalyst evaluation

The monolithic catalysts were used in the partial hydrogenation of sunflower oil at 100 °C, 413 kPa and an agitation rate of 1400 rpm, studying the performance of the catalyst in consecutive tests.

The hydrogenation reactions were carried out in a 600 cm^3 Parr® reactor operated in semi-continuous mode. The monoliths were arranged in the axis of the stirrer (monolithic stirrer, Fig. 1).

Table 2
Composition of the commercial sunflower oil used in the catalytic tests.

Fatty acids	wt%
Palmitic, C16:0	5.9
Stearic, C18:0	3.4
Oleic, C18:1c	39.5
Linoleic, C18:2cc	49.1
Araquidic, C20:0	0.3
Linolenic, C18:3ccc	0.2
Behenic, C22:0	0.7
Total *trans* isomers	<1.0

Table 3
Geometric characteristics of the monolithic catalyst.

Characteristics		
Cylinders length × diameter	cm × cm	1.5 × 14
Geometric volume	cm^3	2.3
Total exposed surface	cm^2	97.5
Cell density	cpsi	350
Surface specified by cell	m^2/cell	3.82
Thickness	mm	0.1

The Pd/Al$_2$O$_3$/Al catalyst was reduced *in situ* (100 °C, 30 min, 100 ml$_{H_2}$/min), and then the oil was introduced into the reactor (previously deoxygenated). When reaction temperature was reached, the H$_2$ pressure was increased to start the reaction. Consecutive tests were performed (without intermediate treatments or activation).

Chromatographic H$_2$ (AGA) and a commercial sunflower oil were used. The composition of the sunflower oil is shown in Table 2. The mass of the Pd catalyst used in all the tests was 2 mg Pd/kg oil. In a set of tests, 65 mg of commercial Ni/SiO$_2$ catalyst (Pricat 9910: 22% Ni, 4% SiO$_2$ dispersed in hydrogenated edible fats) was used as scavenger, while the rest of the operating conditions remained constant.

The analytical studies were carried out chromatographically (AGILENT 4890D) using a flame ionization detector (FID), according to the AOCS Ce 1c-89 norm. A 100 m long SUPELCO 2560 capillary column, with a nominal diameter of 0.25 mm and a nominal film thickness of 0.20 μm, was used for the separation of the different compounds present in the samples. The iodine number, which allows to determine the reaction progress, was calculated from the fatty acid composition following the AOCS Cd 1c-85 norm. The double bond shift is not considered here.

3. Results and discussion

3.1. Characterization of monolithic catalysts

Tables 3 and 4 present the main properties of the monoliths used. During the anodization process, 33.82 g of Al$_2$O$_3$ by square meter of aluminum were generated, and this value was obtained by dissolving the alumina generated with a solution of chromic and phosphoric acid. This amorphous alumina (observed by XRD)

Table 4
Properties of the anodization layer of the monolithic catalyst.

Properties		
Oxide	g Al$_2$O$_3$/m^2 Al	33.82
BET surface area	m^2/g Al$_2$O$_3$	25
BET surface area	m^2/monolith	8
Pore volume	m^3/m^2 Al$_2$O$_3$	2 × 10^{-7}
Pore volume	m^3/monolith	0.5
Pore radius	Å	22
Al$_2$O$_3$ thickness	μm	18
Al$_2$O$_3$ porosity	cm^3/g Al$_2$O$_3$	1.6

provided the monolith with 8 m^2 of surface alumina, with a mean pore size of 45 nm (both values were determined by N$_2$ adsorption isotherms).

Fig. 2A shows a cross-section view SEM micrograph of the aluminum monolith channels. The alumina layer generated on the aluminum monolith was uniform and porous, with a thickness of 18 μm approximately, as shown in Fig. 2B. A close-up of the layer profile shows that the anodic alumina pores are perpendicular to the aluminum surface, as can be seen in Fig. 2C. Fig. 2D shows a SEM top view micrograph of the alumina surface produced. This image shows that the complete surface was covered by regular pores, the diameter of which is in agreement with the difference obtained by N$_2$ adsorption (Table 4). Some large openings or craters can also be observed.

3.2. Catalytic tests

3.2.1. Mass transfer effects

The volumetric gas–liquid mass-transfer coefficient K$_L$a was separately measured (in the 600 cm^3 reactor with the monolithic stirrer) using a physical adsorption method, as described by Dietrich et al. [23]. The value obtained at 100 °C and 1400 rpm was 0.15 s^{-1}, slightly lower than the K$_L$a obtained in the same reactor with a stirrer of inclined blades [28].

The Weisz–Prater criterion (Eq. (1)) was used to evaluate the intraparticle diffusion limitations for both the hydrogen and the triglyceride:

$$\Phi_I = \frac{(-r_{obs,i})\rho_c L^2}{D_{eff,i} C_i} \tag{1}$$

where C_i is the concentration of sunflower oil or H$_2$ [mol/m^3], D_{eff} is the effective diffusion coefficient [m^2/s], L indicates characteristic length [m], $r_{obs,i}$ is the observed rate of double bonds or H$_2$ consumption [mol/s kg$_{cat}$], and ρ_p is the apparent density of the catalyst [kg/m^3]. The effective diffusivity is given as:

$$D_{eff,i} = \frac{D_i . \varepsilon}{\xi} \tag{2}$$

The Weisz–Prater criterion indicates that the mass transfer limitation for the unknown kinetics is negligible when $\Phi_i \ll 1$ [24]. The hydrogen concentration in the liquid was calculated from Fillion and Morsi [30]. Intraparticle diffusion coefficients were taken as $D_{H_2} = 1.2 \times 10^{-8}$ m^2/s [30] and $D_{TAG} = 1 \times 10^{-10}$ m^2/s [25]. The density of sunflower oil was determined from [26] as $\rho_{TGA} = 0.866$ g/ml. The catalyst density was assumed to be 1220 kg/m^3 [27]. The Al$_2$O$_3$ thickness was 18 μm. The alumina tortuosity factor (ξ) was chosen to be 1, because the pore path was a straight line, and the porosity (ε) was estimated to be 2, considering the Al$_2$O$_3$ porosity (1.6 cm^3/g Al$_2$O$_3$) and its density.

In the present experiments, the numerical value of the Weisz–Prater module was 6 for H$_2$ and 0.6 for TAG, indicating that it is not possible to neglect the concentration gradients within the catalyst particle.

3.2.2. Activity and selectivity

The Pd/Al$_2$O$_3$/Al monolithic catalyst was tested in the partial hydrogenation of sunflower oil, at 100 °C and 413 kPa. Conversion is defined as the fraction of the carbon–carbon double bonds that have been hydrogenated with respect to the original amount of double bonds. Fig. 3 shows the C=C conversion at different times of the oil hydrogenation reaction for the first two uses of the monolith.

Initially there was a fast progress of the reaction, reaching a conversion of 50% in 25 min in the case of the first test. For the second reaction, the time needed to reach the same conversion was greater (120 min).
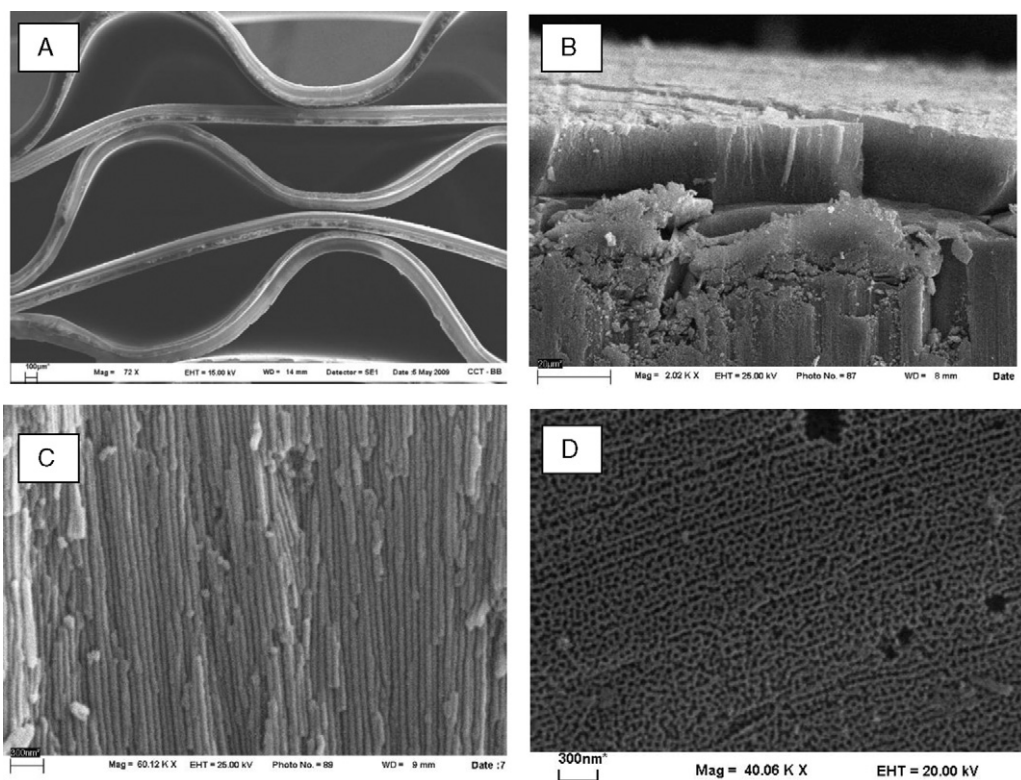
Fig. 2. SEM images. (A) Cross-section view of the aluminum monolith channels (Mag = 72K×), (B) Alumina layer over the aluminum foil (Mag = 2.02K×), (C) Lateral view of pores in the alumina layer (C: Mag = 60.12K×, D: 80K×), (D) Top view of the porous surface of the alumina obtained by anodization (Mag = 40.06K×).

The catalytic activity was very high. In order to compare this value with that of similar catalysts, it can be indicated that when using a 0.78 wt% Pd/γAl$_2$O$_3$ powder catalyst with 60% dispersion [28], at equal temperature and pressure, with a little higher Pd:oil ratio (8 mg Pd/kg oil), a conversion of 20% was reached at 20 min, and of 45% at 60 min of reaction. A 5 wt% Pd/carbon catalyst, operating under similar conditions (5 mg Pd/kg oil, 93 °C), showed a comparable activity [9]. When a Pd/Al$_2$O$_3$–cordierite and Pd/Al$_2$O$_3$–Fecralloy monolithic catalysts (3.8 wt% of Pd, with a 37% dispersion) were studied in the same reaction, at equal operating conditions (33 mg Pd/kg oil), a 20.9% and 18.7% conversion was observed at 2 h of reaction time [16].Plourde et al. [7] reported that a cordierite monolith with palladium as the active component (no

other details are given) used in the hydrogenation of bleached soybean oil (96–120 °C and 0.9–2 MPa) showed a conversion of 40% in 120 min (calculated from the values presented in their work).

Fig. 4 presents the product distribution as a function of C=C conversion. As indicated above, the double effect of hydrogenation is the reduction of unsaturated compounds or their modification to form *trans* isomers. The results can be understood in view of the reaction network. The overall hydrogenation reaction involves the consecutive saturation of *cis*-C18:2 to *cis*-C18:1 and its subsequent saturation to C18:0, as well as the parallel isomerization of *cis*-C18:2 to *trans*-C18:2 and *cis*-C18:1 to *trans*-C18:1. The reaction pathway could also involve the hydrogenation of *trans*-C18:2 to *cis*-C18:1 and *trans*-C18:1 to C18:0. The concentration of the fatty acid
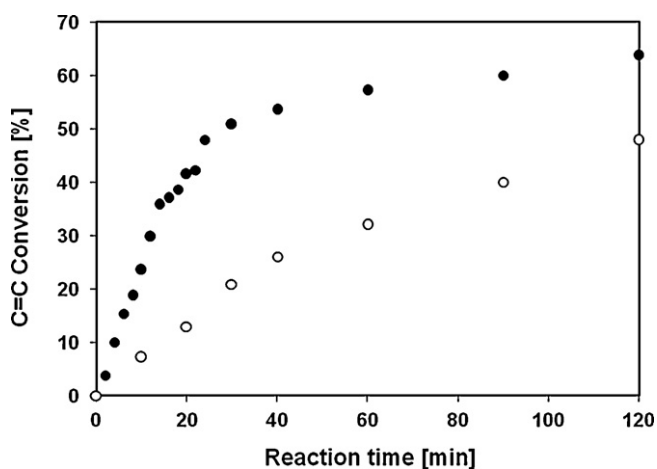

Fig. 3. Double bond conversion versus reaction time for the hydrogenation of sunflower oil at 100 °C and 413 kPa over Pd/Al$_2$O$_3$/Al. Reference: first use (●); second use (○).
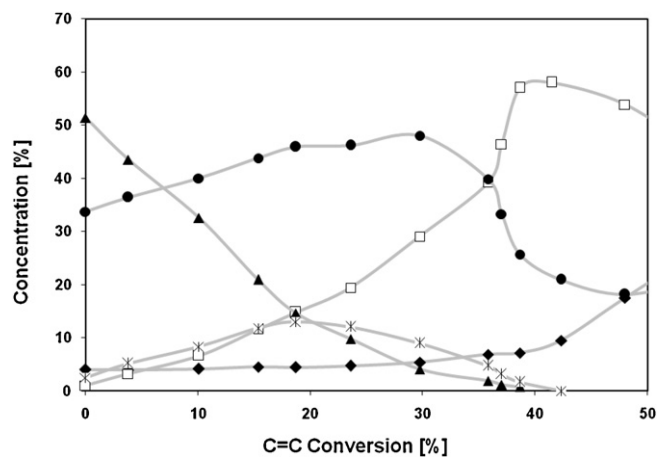

Fig. 4. Product distribution for the hydrogenation of sunflower oil at 100 °C and 413 kPa over Pd/Al$_2$O$_3$/Al. References: (●) *cis*-C18:1c, (▲) *cis*-*cis*-C18:2, (♦) C18:0, (□) *trans*-C18:1t, (∗) *trans*-C18:2 (first use of the monolith).
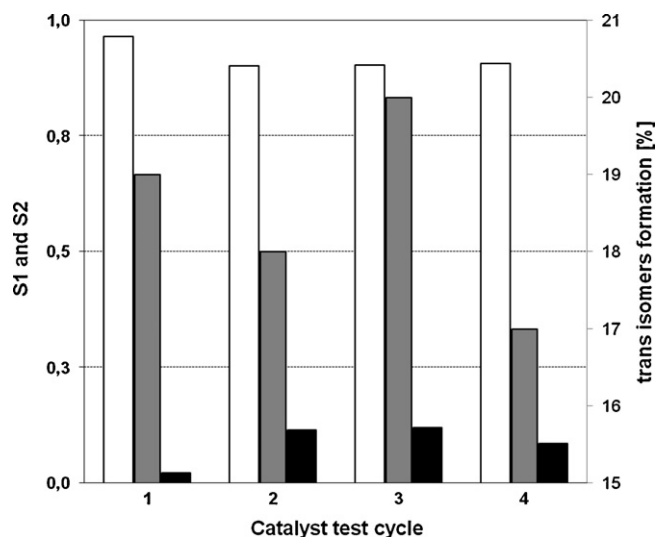
Fig. 5. Selectivities S_1 and S_2, and *trans* isomer concentration for a conversion of 20%, for four consecutive tests. References: (□) S_1, (■) S_2, (■) *trans* isomers (%). $S_1 = (C18:1-C18:1_o)/(C18:2_o-C18:2)$. $S_2 = (C18:0-C18:0_o)/(C18:1-C18:1_o)$.

C18:3 is not reported in Fig. 4 because it is very low in sunflower oil.

Using Pd catalysts, a lower production of C18:0 is attributed to the difference in the affinity of C18:2 and C18:1 and their stronger adsorption on the dispersed Pd, thus favoring the formation of C18:1 rather than C18:0 [28,29].

It is evident in Fig. 4 the high formation of *trans* isomers at the expense of the consumption of *cis*-C18:1. It can be observed that the formation of C18:0 increased with the consumption of *trans*-C18:1, indicating that it was especially favored the path of the reaction:

$$cis\text{-}C18:1 \rightarrow trans\text{-}C18:1 \rightarrow C18:0$$
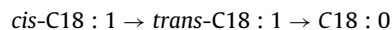
This result can be related to mass transfer problems inside the catalyst pores. The hydrogen concentration in oil is very low ($9.3\,mol/m^3$, calculated from the data reported by Fillion and Morsi [30]), and its diffusion through the catalyst pores to the active site is difficult. The reaction selectivity of hydrogenation versus isomerization depends heavily on the hydrogen availability on the surface catalyst [28,29]. When there are not limitations for the H_2 molecule to reach the Pd, an excess of hydrogen will exist on the active site, and the double bond in the triglyceride molecule will tend to saturate before the isomerization. However, when the restrictions on the hydrogen are significant, a higher amount of *trans* isomer compounds will be produced. When there is no hydrogen on the surface, both reactions stop.

Fig. 5 shows selectivity S_1 and S_2 for four consecutive tests and a conversion of 20%. S_1 is defined as the amount of monounsaturated fatty acids (C18:1) formed with respect to the amount of diunsaturated fatty acids converted (C18:2), and selectivity S_2 is the amount of saturated fatty acids (C18:0) produced with respect to the amount of monounsaturated fatty acids (C18:1) converted.

S_1 had little variation (between 0.96 and 0.91) and the value indicates that the formation of *cis* monounsaturated products/compounds was favored equally in all the uses. The value of S_2 increased in the second use with respect to the first, and then remained constant (0.02 and 0.12).

Fig. 8 also shows the formation of *trans* isomers (total amount of *trans* carbon–carbon double bonds in the products) at 20% conversion. The *trans* isomer content remained fairly constant, between 16% and 20%, in the consecutive tests. This value is slightly higher than that found by our group for Pd/Al$_2$O$_3$–cordierite and Pd/Al$_2$O$_3$–Fecralloy monolithic catalysts (12.8%) or a powder
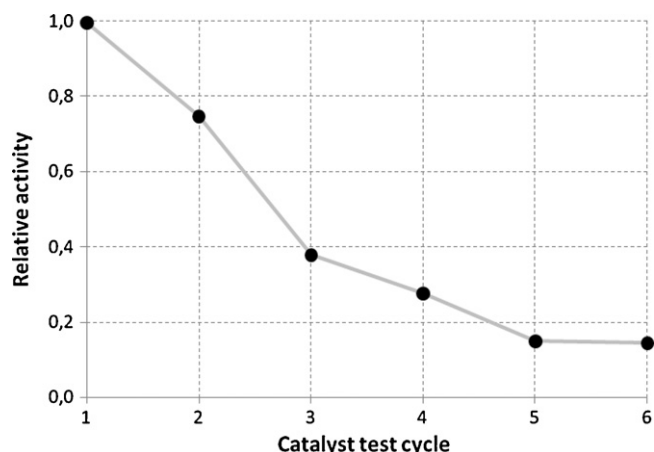

Fig. 6. Relative activity of a Pd/Al$_2$O$_3$/Al monolithic catalyst used in subsequent hydrogenation batches.

Pd/γAl$_2$O$_3$ (16.2%) at equal operating conditions and double bond conversion [16]. Subsequent consecutive tests for the three samples did not show significant variations regarding selectivity.

Pérez-Cadenas [17,18], using a palladium supported over nonporous-carbon coated monolith in the hydrogenation of fatty acid methyl esters, found a 13.8% of total amount of *trans* isomers (8.5% *trans*-C18:1 and 5.3% *trans* isomers of linoleate) at 20% double bond conversion.

3.2.3. Stability and regeneration of the monolithic catalyst

The stability of the catalyst activity and selectivity through the consecutive uses is very important for a structured catalyst, because one of its main characteristics is the possibility to separate it easily from the reaction media, and use it repeatedly.

Multiple consecutive tests were made with the monolithic catalyst in order to examine the effects of reuse on activity and stability. No treatment was performed in the samples between tests, only Pd oxidation was avoided.

Fig. 6 shows the relative conversion reached, and that the relative catalyst activity decreased for each use.

The values correspond to the conversion for a reaction time of 2 h and $250\,cm^3$ of oil to be processed by batch. In the first reactions, a sharp decrease in activity was observed, but the values remained above ~25% until the fourth use. Then the activity loss rate diminished until it became stabilized. This behavior is typical in this kind of catalytic systems [4,16], although in this case it was more pronounced. The long reaction time to which the sample was exposed in each test, reaching high levels of hydrogenation of oil, must be pointed out. Boger et al. [4] found that the activity decreased in the first two batches to approximately 55% of the initial activity. After the third batch, no further change in activity was observed. However, the cause for the catalyst deactivation is not fully understood, and the authors infer that a significant part of the deactivation is probably due to coking of the most active sites, as they were able to partially recover activity after regenerating the catalyst in a hydrogen atmosphere at elevated temperature (not shown in the article).

Sánchez M. et al. [16] observed that after three consecutive tests, a Pd/Al$_2$O$_3$–cordierite monolith showed no change in activity or selectivity, whereas a Pd/Al$_2$O$_3$–Fecralloy monolith showed a partial deactivation (10%), which was attributed to a loss of catalytic material.

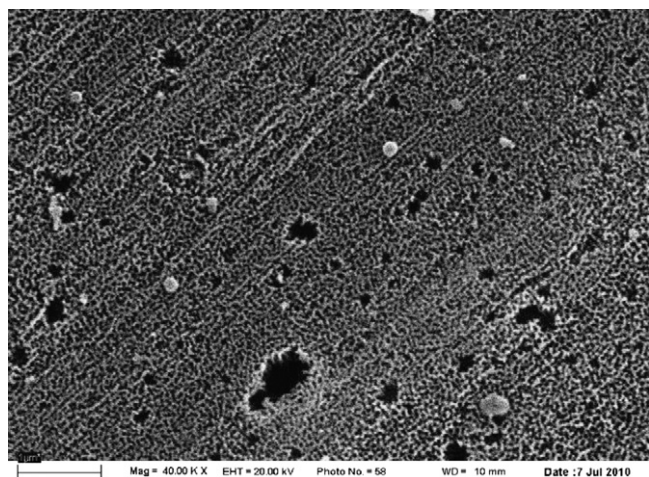In order to try to recover the activity of the samples, the monoliths (with three and ten previous uses) were:

Fig. 7. SEM micrograph of the alumina surface in a monolith used 10 times in reaction (Mag = 40,000×).

1. Washed in hexane twice at 60 °C in a Parr reactor, at 800 rpm for 45 min.
2. Washed in hexane and calcined (500 °C for 2 h, with a heating ramp rate of 2 °C/min).

With the samples thus pre-treated, the catalytic tests were performed under the usual operating conditions. In none of the cases was the activity recovered. No changes were observed in the values of selectivities S_1 and S_2.

The causes of the catalyst deactivation can be many:

1. Detachment of the alumina.
2. Physical obstruction of the pores by the accumulation of saturated product.
3. Active site poisoning.
4. Coke formation.

In order to verify if the alumina layer detached from the catalyst, the surface of a monolith washed in hexane (at 60 °C, three times) was analyzed by SEM. Fig. 7 presents the SEM micrograph of the alumina surface, and it can be observed that the pore distribution and size is very similar to that found in the unused monolith (Fig. 2D). No change in morphology or loss of alumina layer was found in none of the analyzed areas. For this reason, the hypothesis that the monolith deactivation occurs due to catalyst loss by detachment of the alumina layer is disregarded.

In Fig. 7, little spheres of a solid can be observed, probably reaction residues that remained on the alumina surface, even after the monoliths were washed in hot hexane. This residue was studied by DRIFT. Fig. 8 shows the IR spectra obtained for the surface of the unused monolith, the washed monolith, the calcined monolith, and the volatile residue that remained adhered to the glass tube in which the monolith calcination was performed. The IR spectra for the pure and hydrogenated sunflower oil are also presented as a reference. In spectra C–F, aliphatic groups are found. The most important vibrational modes are the C–H stretching around 3000 cm^{-1} and the –CH deformation modes around 1460 cm^{-1} and 1380 cm^{-1}. In the same spectra, aliphatic ester groups are presented by signal close at 1750 cm^{-1} (C=O stretch) and 1250 cm^{-1} (C–O stretch). In spectra A and B, the band at 1460 also indicates the –C=O functional group.

In spectrum F (hydrogenated oil), the signal at 970 cm^{-1} is characteristic of *trans* olefins. In spectrum E (sunflower oil), signals at 3008 and 1655 cm^{-1} are typical of *cis* olefins.
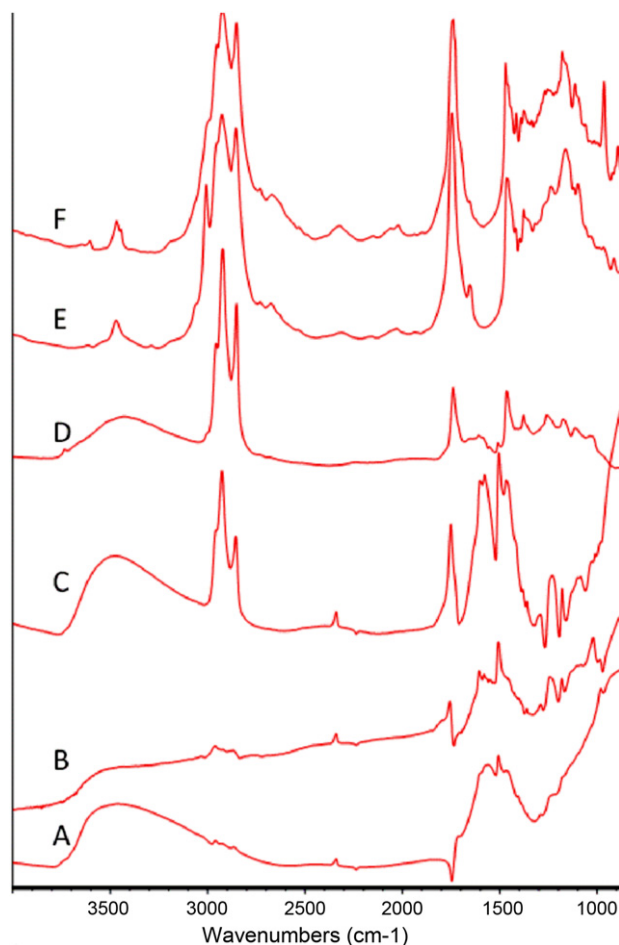

Fig. 8. IR spectra (A) unused monolith, (B) calcined monolith, (C) washed monolith, (D) volatile residue from calcination, (E) sunflower oil, (F) hydrogenated sunflower oil.

A broad –OH absorption peak around 3500 cm^{-1} is presented in spectra A and C, but is barely noticeable in the calcined monolith (spectrum B).

These observations indicate that the reaction residues remained on the surface of the washed monolith, and thus the lack of activity in the washed monolith can be attributed in part to the physical obstruction of the catalyst pores by the accumulation of saturated product. The volatile residue recovered from the calcination treatment showed an IR spectrum similar to that of hydrogenated oil.

In order to verify if the decrease in activity occurs due to poisoning of the active site by adsorption of minor components present in the oil (i.e. phospholipids, close to 5 ppm [31]), three consecutive reaction tests were performed adding 65 mg of commercial Ni/SiO$_2$ catalyst (66 mg Ni/Kg oil) used as scavenger, while the Pd:oil ratio and the rest of the operating conditions remained constant. Ni/SiO$_2$ was selected as scavenger taking into account the work of Diosady and co-workers [32]. They reported that the addition of Ni increased the hydrogenation activity of a 5% Pd/γAl$_2$O$_3$ catalyst, although a 23% Ni catalyst was inactive under equal operating conditions. The increased activity of the Pd/Ni system over Pd alone was attributed to the adsorption of catalyst poisons from the oil by Ni.

A catalytic test only with Ni was performed, and it was verified that under the present operating conditions the C=C conversion was negligible.

The double bond conversion, S_1 and S_2 selectivities and *trans* isomer production found for three consecutive tests were similar to those found for the catalytic tests without Ni. The presence of Ni

in high concentrations with respect to Pd (Ni:Pd molar ratio = 60) did not alter the gradual deactivation of the Pd/Al$_2$O$_3$/Al catalyst, indicating that deactivation did not occur by poisoning.

In order to analyze if deactivation occurs due to coking of the most active sites, the surface of the monolith used in reaction 10 times, washed in hexane and calcined (500 °C for 2 h) was analyzed by DRIFT. As shown in spectrum B of Fig. 8, signals of low intensity were found around 3000 cm^{-1} corresponding to C–H stretching, which could indicate that a small amount of carbonaceous residues remained on the surface. This may also include reactants strongly adsorbed on the metal or on the support, as well as the more dehydrogenated species present on the catalyst.

This result is in agreement with those reported by Edvardsson et al. [33]. They investigated the Pd and Pt catalyst deactivation supported on α- and γ-Al$_2$O$_3$ by coke formation during hydrogenation of vegetable oil in liquid phase. It was found that only Pd/γ-Al$_2$O$_3$ deactivated during the hydrogenation process. This catalyst lost more than 50% of its initial activity after four batch experiments. A mechanism was suggested where conjugated dienes, which are formed to a larger extent on Pd than on Pt, were responsible for the formation of the coke that deactivated the catalyst.

4. Conclusions

Monolithic catalysts of anodized aluminum were prepared and characterized. It was shown that these structures can be a good alternative as structured catalysts in the reaction of partial hydrogenation of sunflower oil, intended to simplify the industrial process.

The monolithic Pd/Al$_2$O$_3$/Al catalysts showed to be active, with a 50% C=C conversion in 30 min. When consecutive tests were performed, a loss of activity was observed, decreasing 80% in the sixth test, which is attributed to the presence of carbonaceous residues. Regeneration of spent monolith was also studied, but no suitable solvent or method was found at this point of the research.

Acknowledgements

References

[1] J. Coenen, Hydrogenation of edible oils, J. Am. Oil Chem. Soc. 53 (1976) 382.
[2] N. Nikolaou, C. Papadopoulos, A. Lazaridou, A. Koutsoumba, A. Bouriazos, G. Papadogianakis, Catal. Commun. 10 (2009) 451.
[3] R. Yang, M. Su, M. Li, J. Zhang, X. Hao, H. Zhang, Bioresour. Technol. 101 (2010) 5903.
[4] T. Boger, M.M.P. Zieverink, M.T. Kreutzer, F. Kapteijn, J.A. Moulijn, W.P. Addiego, Ind. Eng. Chem. Res. 43 (2004) 2337.
[5] R.E. Albers, M. Houterman, T. Vergunst, E. Grolman, J. Moulijn, AIChE J. 44 (1998) 2459.
[6] E. Santacesaria, P. Parrella, M. Di Sergio, G. Borrelli, Appl. Catal. A 116 (1994) 269.
[7] M. Plourde, K. Belkacemi, J. Arul, Ind. Eng. Chem. Res. 43 (2004) 2382.
[8] V.I. Saychenko, I.A. Makaryan, Platinum Met. Rev. 43 (1999) 74.
[9] J. Ray, J. Am. Oil Chem. Soc. 62 (1985) 1213.
[10] G. Mangnus, A. Beers, "Hydrogenation of oils at reduced TFA content," Oils & Fats International 20: 33–35, DMG World Media (UK) Ltd. (2004).
[11] T.A. Nijhuis, A.E.W. Beers, T. Vergunst, I. Hoek, F. Kapteijn, J.A. Moulijn, Catal. Rev. 43 (4) (2001) 345.
[12] T.H. Elmer, US Patent 3,958,058 (1976).
[13] T. Nijhuis, M. Kreutzer, A. Romijn, F. Kapteijn, J. Moulijn, Chem. Eng. Sci. 56 (2001) 823.
[14] H. Marwan, J.M. Winterbottom, Catal. Today 97 (2004) 325.
[15] S. Irandoust, B. Andersen, Chem. Eng. Sci. 43 (1988) 1983.
[16] J.F. Sánchez M., O.J. González, M. Montes, G.M. Tonetto, D.E. Damiani, Catal. Commun. 10 (2009) 1446.
[17] A.F. Pérez-Cadenas, M.M.P. Zieverink, F. Kapteijn, J.A. Moulijn, Carbon 44 (2006) 173.
[18] A.F. Pérez-Cadenas, F. Kapteijn, M.M.P. Zieverink, J.A. Moulijn, Catal. Today 128 (2007) 13.
[19] R. Hayes, S. Kolaczkowski, W. Thomas, Comp. Chem. Eng. 16 (1992) 645.
[20] A. Cybuslki, J.A. Moulijn, Catal. Rev. Sci. Eng. 36 (1994) 179.
[21] L. Wang, M. Sakurai, H. Kameyama, J. Chem. Eng. Jpn. 37 (2) (2004) 1513.
[22] N. Burgos, M. Paulis, M. Montes, J. Mater. Chem. 13 (2003) 1458.
[23] E. Dietrich, C. Mathieu, H. Delmas, J. Jenck, Chem. Eng. Sci. 47 (1992) 3597.
[24] H. Fogler, L. Scott, Elements of Chemical Reaction Engineering, 3rd ed., Prentice Hall, New Jersey, 1999.
[25] K. Andersson, M. Hell, L. Löwendahl, N.-H. Schöön, J. Am. Oil Chem. Soc. 51 (1974) 171.
[26] D. Swern (Ed.), Bailey's industrial oil and fat products, Catal. Commun. vol. 2, 4th ed. (1982).
[27] J.M. Smith, Chemical Engineering Kinetics, 3rd ed., McGraw-Hill Science/Engineering/Math, 1981.
[28] M. Fernández, M.J. Sánchez, G. Tonetto, D. Damiani, Chem. Eng. J. 155 (2009) 941.
[29] Y. Kitayama, M. Muraoka, M. Takahashi, T. Kodoma, H. Itoh, E. Takahashi, M. Okamura, J. Am. Oil Chem. Soc. 73 (1996) 1311.
[30] B. Fillion, B.I. Morsi, Ind. Eng. Chem. Res. 39 (2000) 2157.
[31] O. Zufarov, S. Schmidt, S. Sekretár, Acta Chim. Slovaca 1 (2008) 321.
[32] A.J. Wright, A. Wong, L.L. Diosady, Food Res. Int. 36 (2003) 1069.
[33] J. Edvardsson, P. Rautanen, A. Littorin, M. Larsson, J. Am. Oil Chem. Soc. 78 (2001) 319.